ApoE-modified solid lipid nanoparticles: A feasible strategy to cross the blood-brain barrier

Author links open overlay panelR.Dal Magro[a]
F.Ornaghi[b1]I.Cambianica[b]S.Beretta[b]F.Re[a]C.Musicanti[c]R.Rigolio[d]E.Donzelli[d]A.Canta[d]E.Ballarini[d]G. Cavaletti[d]P.Gasco[c]G.Sancini[a]
https://doi.org/10.1016/j.jconrel.2017.01.039

Abstract

Solid lipid nanoparticles (SLN) are colloidal drug delivery systems characterized by higher entrapment efficiency, good scalability of the preparation process and increased sustained prolonged release of the payload compared to other nanocarriers. The possibility to functionalize the surface of SLN with ligands to achieve a site specific targeting makes them attractive to overcome the limited blood-brain barrier (BBB) penetration of therapeutic compounds. SLN are prepared for brain targeting by exploiting the adaptability of warm microemulsion process for the covalent surface modification with an Apolipoprotein E-derived peptide (SLN-mApoE). Furthermore, the influence of the administration route on SLN-mApoE brain bioavailability is here evaluated. SLN-mApoE are able to cross intact a BBB in vitro model. The pulmonary administration of SLN-mApoE is related to a higher confinement in the brain of Balb/c mice compared to the intravenous and intraperitoneal administration routes, without inducing any acute inflammatory reaction in the lungs. These results promote the pulmonary administration of brain-targeted SLN as a feasible strategy for improving brain delivery of therapeutics.

Graphical abstract

Solid lipid nanoparticles (SLN), prepared by warm microemulsion, are functionalized with a brain targeting peptide (mApoE). Intratracheally instilled SLN-mApoE translocate from the lungs to the brain crossing the blood-brain barrier.

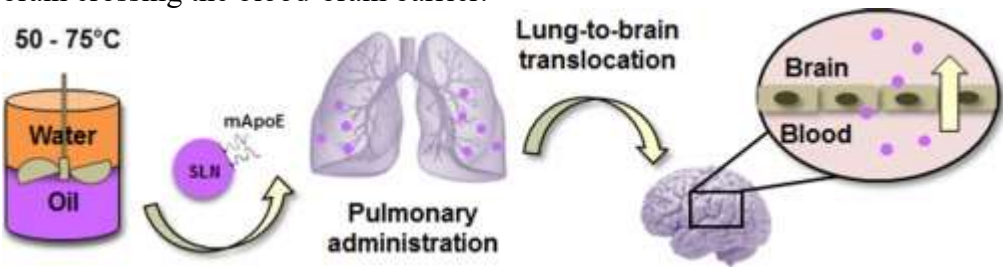

1. Download : Download high-res image (90KB)
2. Download : Download full-size image

- **Previous** article in issue
- **Next** article in issue

Keywords

Solid lipid nanoparticles
ApoE-derived peptide
Pulmonary administration
Brain targeting
Blood-brain barrier

1. Introduction

In the last decades, nanotechnologies have continuously evolved, raising great interest in pharmacological and biomedical field [1]. Recent applications in nanomedicine focus on nanoparticles (NPs) as they are promising tools for site-specific delivery of drugs and diagnostic agents, through the possibility to functionalize their surface with target-specific ligands (active targeting). Nowadays, brain drug development remains a challenging task due to the presence of the blood-brain barrier (BBB), a very restrictive barrier mainly composed of tightly sealed endothelial cells [2], [3]. Indeed, due to its anatomy and physiology, the BBB strictly regulates the brain access and clearance of endogenous and exogenous molecules from the systemic circulation [4], [5]. During the last three decades, different approaches have been developed to circumvent the BBB. Among others, embedding drugs within nanoparticulate matter able to cross the BBB is considered one of the most promising [6], [7], [8]. Solid lipid nanoparticles (SLN) are very interesting colloidal systems that have been studied for almost twenty years [9]. Historically, the origin of SLN can be traced back to the introduction in clinics of lipid emulsions for parenteral nutrition in the 1970s. Comparing to precursor oil based emulsions, SLN are aqueous nanoscale suspensions prepared mainly with phospholipids and solid lipids, such as fatty acids or triglycerides, phospholipids or synthetic surfactants with good physiological tolerability [2], [10]. These ingredients are generally considered safe, biocompatible and biodegradable [10], [11]. Moreover, they provide better colloidal stability thus creating the opportunity for sustained drug release and reducing the dosing and the frequency of the treatment [12], [13]. Compared with liposomes, SLN have a higher stability, may incorporate both lipophilic and hydrophilic drugs and scalable production methods are already available [14]. Moreover, for the preparation of SLN neither organic solvents nor expensive excipients are needed as in the case of polymeric NPs [13].

Among the possible preparation methods available nowadays for SLN production, warm microemulsion technique focuses on specific set up of composition of the interface between lipids and water: this process allows great flexibility in design of surface characteristics of the final product and lets the introduction of different functional groups to be used for further bio-conjugation of SLN with targeting ligands. Stealth agents such as PEG-derivatized lipids are commonly used to obtain sterically stabilized SLN to avoid recognition by macrophages and to prolong the circulation time of SLN [15], [16]. Several colloidal systems have been designed for CNS targeting by exploiting specific surface modifications with targeting ligands capable of taking advantage of specific receptors or nonspecific pathways [17], [18], [19]. Nevertheless, it has been widely emphasized the efficacy of the surface modification with less attention given to the comparison between the results obtained by administering the colloidal systems by different routes [20]. Although delivery to the blood circulation has the potential benefit of providing access to any vascularized tissue in the body, this pervasive approach also increases the likelihood that unintended tissues will be targeted. It is typically observed that systemic delivery of nanoparticles results in substantial accumulation in both the liver and the spleen as a result of immune clearance by the mononuclear phagocyte system. This off-target accumulation is a major impediment to achieving specificity with systemic delivery [21]. SLN have been virtually proposed for all

administration routes [22] e.g., parenteral [23], oral [24], dermal [25] and ocular [26]. Among the different administration routes, pulmonary delivery is a field of increasing interest not only for the local treatment of airway diseases but also for the systemic administration of drugs [27]. Indeed lungs are an attractive target for the pulmonary administration of active pharmaceutical ingredients in the form of various drug delivery systems [12], [28], [29], [30]. Additionally, this route offers many advantages over conventional per oral administration, such as the circumvention of the first pass effect and a high surface area with rapid absorption due to an extensive vascularization [31], [32]. Since the capability of a synthetic decapeptide derived from the receptor binding region of human apolipoprotein E (mApoE) to enhance liposomes (LIP) penetration in the central nervous system (CNS) has already been demonstrated, [33], [34], [35] as well as the feasibility of the pulmonary administration of mApoE-functionalized LIP as an efficient strategy to reach the brain [36], this work aims at optimizing the preparation of SLN for brain drug targeting by exploiting the pulmonary route. We evaluated the adaptability of warm microemulsion process for ligand surface modification of SLN with mApoE to target the BBB. Moreover, we investigated how the different administration routes affected the SLN-mApoE brain bioavailability.

2. Materials and methods

2.1. Materials

Dynasan 116 was a gift from Cremer Oleo Division (Hamburg, Germany), epikuron 200 (soybean lecithin with a phosphatidylcholine content of at least 92% - Cargill) was purchased from AVG (Italy), sodium taurocholate (bile salt) was purchased from PCA (Italy), 1-butanol was purchased from Carlo Erba (Milan, Italy). 1,2-Distearoyl-sn-*glycero*-3-phosphoethanolamine-*N*-[maleimide(polyethylene glycol)-2000] (DPM) and 1,2-dipalmitoyl-sn-*glycero*-3-phosphatidic acid sodium salt (DPPA) were purchased from NOF Corporation (Tokyo, Japan). [^{14}C]-Sucrose, [^{3}H]-cholesteryl hexadecyl ether (CE), [^{14}C]-DPPA and Ultima Gold scintillation cocktail were from PerkinElmer (Italy). l-Cysteine HCl was purchased from Thermo Fisher Scientific (Waltham, MA, USA). 3,3′-Dioctadecyloxacarbocyanine perchlorate (DiO) and 1,1′-Dioctadecyl-3,3,3′,3′-Tetramethylindotricarbocyanine Iodide (DiR) dyes were from VWR (Italy). Transwell permeable supports 0.4 μm polyester membrane 12 mm insert, 12 well plates, were from Corning (NY, USA). All the media and supplements for cell culture were purchased from Life Technologies, Thermo Fisher Scientific. Phalloidin was from Molecular Probes, Thermo Fisher Scientific. Rabbit anti-LAMP1, rabbit anti-Niemann Pick C1 and rabbit anti-Rab11 antibodies were from Abcam (Science Park, Cambridge, UK). Mouse anti-EEA1 was from BD Transduction laboratories (BD Biosciences, San Jose, CA, USA). IT instillation was performed using a MicroSprayer Aerosolizer system (Penn Century, USA). All other chemicals were purchased from Sigma-Aldrich.

2.2. Preparation of SLN

SLN were prepared by Nanovector srl (Turin, Italy) by oil/water warm microemulsion technique. The microemulsion was prepared at 60–64 °C by heating dynasan 116, epikuron 200, short chain alcohols, and then adding an aqueous solution of bile salts heated at the same temperature. The warm microemulsion was dispersed in cold water to obtain an aqueous dispersion of SLN. The surface of SLN was functionalized with DPM to perform conjugation with the peptide CWG-LRKLRKRLLR (mApoE; residues 141–150 of human apolipoprotein E) exploiting thiol-maleimide reaction, by substituting 0.4% molar percentage of phosphatidylcholine (PC) with the compound. The peptide CWG was added at the C-term of mApoE to assess the yield of coupling reaction. Fluorescent SLN were prepared by adding the fluorescent lipophilic probes DiO (λex\λem = 484\501 nm) or DiR (λex\λem = 750\780 nm) to the oil phase of the microemulsion.

Dually radiolabelled SLN were prepared using two radioactive compounds: [^{3}H]-CE and [^{14}C]-DPPA (. SLN incorporating fluorescent probes or radioactive markers were purified by tangential ultrafiltration (repeated four times) and using Vivaflow 50 system (Sartorius, Germany) equipped with regenerated cellulose membrane 100000 MWCO.

2.3. Preparation and characterization of SLN functionalized with ApoE peptide

Fluorescent and radiolabelled SLN were incubated with 50 µM mApoE overnight at 4 °C, protected from light. The final mApoE:DPM molar ratio was 1:1. After the incubation, the reaction mixture was purified by tangential ultrafiltration to remove unbound peptide by using a 300 kDa membrane. The yield of coupling reaction between SLN and mApoE was assessed by fluorescence spectroscopy of tryptophan residue at the C-terminal of mApoE, as previously described [29]. As a control, SLN-cys were prepared by incubating the SLN dispersion with cysteine in order to block maleimide reactive site. SLN were characterized in terms of dimension, ζ-potential and polydispersity index by means of Dynamic Light Scattering (DLS) analysis.

2.4. Culture of hCMEC/D3 cells

Human cerebral microvascular endothelial cells (hCMEC/D3) were obtained from Institut Cochin (INSERM, Paris, France). Cells at passage between 27 and 37 were grown on tissue culture flasks, covered with 0.1 mg/mL rat tail collagen type 1, in EBM-2 medium supplemented with 5% fetal bovine serum (FBS), 1% Penicillin-Streptomycin, 1.4 µM hydrocortisone, 5 µg/mL ascorbic acid, 1/100 chemically defined lipid concentrate, 10 mM HEPES and 1 ng/mL basic fibroblast growth factor (FGF). Cells were seeded at a density of 24,000–33,000 cells/cm^{2} and cultured at 37 °C, 5% CO_2. For permeability assays, cells were seeded on 12-well transwell inserts coated with rat tail collagen type 1; cell culture medium was changed every 2 days. For uptake studies by confocal microscopy, hCMEC/D3 were grown on 25 mm glass coverslips pre-coated with collagen; confluent hCMEC/D3 monolayers were obtained typically by day 3. For flow cytometry analysis, cells were cultured on type 1 collagen-coated 12-wells plates; confluent hCMEC/D3 monolayers were obtained typically by day 3.

2.5. Cytotoxicity assay

Cell viability was assessed by means of PrestoBlue assay (Invitrogen). hCMEC/D3 were incubated with SLN-cys or SLN-mApoE at the final lipid concentrations of 0.05 mg/mL, 0.1 mg/mL, 0.5 mg/mL or 1 mg/mL at 37 °C, 5% CO_2. After 24 h, culture medium was removed, PrestoBlue solution was added to each well and incubated at 37 °C. Absorbance was measured at different time points until a plateau was reached. Values were measured as OD readings at 570/600 nm using FLUOStar Omega Multidetection Microplate reader (BMG LABTECH).

2.6. Time dependent nanoparticle-cell-interaction

hCMEC/D3 were incubated with SLN-cys or SLN-mApoE loaded with 0.4 µM DiO at the final total lipid concentration of 0.1 mg/mL for up to 5 h at 37 °C. At different time points, cells were prepared for fluorescence-activated cell sorting (FACS) analysis. Data corresponding to 20,000 events in a user-determined area were collected for every experimental condition. Samples were analysed using DIVA software on a FACSCanto I (BD Biosciences, San Jose, California).

2.7. Intracellular distribution of SLN by confocal microscopy in hCMEC/D3

Cells were incubated with DiO-loaded SLN (0.4 μM DiO, 0.1 mg/mL of total lipids) at 37 °C for 3 h or overnight, and fixed in 10% formalin solution. Subcellular compartments were stained by immunofluorescence technique and the images were analysed by confocal laser scanning microscopy (CLSM), as described [36]. Colocalization analysis was performed using ImageJ-based intensity correlation analysis. Auto setting was used to regulate the thresholds for red and green channels.

2.8. Pathways involved in the cellular uptake of SLN-mApoE

hCMEC/D3 were pre-incubated with the following endocytosis inhibitors: amiloride (100 μM), filipin (3 μM) or chlorpromazine (30 μM) for 30 min. Then, the medium was removed and fresh medium containing DiO-loaded SLN-mApoE (0.4 μM DiO, 0.1 mg/mL of total lipids) and inhibitors was added. After 3 h, cells were prepared for FACS analysis. As a control, cells incubated with SLN-mApoE without any inhibitor were used.

2.9. Endothelial permeability of radiolabelled SLN

hCMEC/D3 were seeded in 12-well transwell inserts (polyester membrane; 0.4 μm pore size) coated with rat tail collagen type 1 at a density of 62,500 cells/cm^2. Experiments were usually performed at day 14 after seeding, when a constant transendothelial electrical resistance (TEER) value, measured using an EVOM Endohm chamber (World Precision Instruments), was obtained. Dually radiolabelled SLN-cys or SLN-mApoE at the final total lipid concentration of 0.1 mg/mL ([^{3}H]-CE = 2.48 × 10^{-8} Ci, [^{14}C]-DPPA = 6.31 × 10^{-9} Ci) were added in the upper chamber of the transwell system. Samples were taken from the lower compartment at different time points (60 and 180 min) and the radioactivity was measured using a Tri-Carb 2200 CA Liquid Scintillation Analyzer (Packard). Transendothelial permeability (EP) was calculated as previously described [35], [37]. The efflux of the hydrophilic marker [^{14}C]-sucrose (200 μM) added in the upper chamber was measured to evaluate the paracellular permeability of hCMEC/D3 monolayer.

2.10. Animals

Male Balb/c mice (6–8 weeks old) were purchased from Harlan Laboratories (Italy). Mice were housed in plastic cages under controlled environmental conditions (temperature 19–21 °C, humidity 40–70%, lights on 12 h/day); food and water were administered ad libitum. To avoid interferences during fluorescence detection animals were fed with chlorophyll-free food started from 72 h before the treatment. All the experiments were performed in mice under controlled general anaesthesia (isoflurane 2.5% - O_2 70% - NO_2 30%) to avoid pain and discomfort. The established rules of animal care approved by Italian Ministry of Health (DL 116/92) were followed; the protocol was approved by the Institutional Animal Care and Use Committee of the University of Milano-Bicocca.

2.11. In vivo administration of SLN

The bioavailability of SLN to the brain was evaluated by means of FMT1500™ Fluorescence Molecular Tomography system (Perkin Elmer). Intraperitoneal (IP) administration, intravenous (IV) injection and intratracheal (IT) instillation were performed on mice kept under anaesthesia during the whole administration and fluorescence detection procedure (n = 10 per group). For each administration route, SLN loaded with 40 μM DiR at the final total lipid concentration of 10 mg/mL were used. Five animals per group were treated with 50 μL of SLN-cys, the other five mice with 50 μL of SLN-mApoE. IT instillation was performed using a MicroSprayer Aerosolizer system (Penn Century, USA). After SLN administration, anesthetised mice were placed into the imaging cassette inside the chamber of the instrument. The total amount (in picomoles) of fluorophore in a

selected three-dimensional region of interest (ROI) was calculated by the TrueQuant software using previously generated standards of the appropriate dye [38]. ROI were drawn in a blind manner by an operator unaware of the experimental origin of the specimens in order to eliminate any operator bias. Every mouse was analysed 10 min, 1 h, 3 h and 24 h after the administration. A group of 6 animals (2 mice for each administration route) was treated with 50 μL of DiR and used as a control. During the whole experiment, no changes in animal weight and behaviour were observed.

2.12. Bronchoalveolar lavage fluid analysis

24 h after IT instillation, 5 mice treated with 50 μL of isotonic saline solution (sham) and 5 mice treated with 50 μL of SLN-mApoE were euthanized by cervical dislocation and the bronchoalveolar lavage (BAL) fluid was collected and processed, as previously described [39]. Supernatants were stored for biochemical analysis, while pellets were collected for cell counts.

2.12.1.1. Cell counts

Pellets collected from BAL fluids were resuspended in Dulbecco's Modified Eagle Medium (DMEM) and were used for cell differential count as previously described [39].

2.12.1.2. Cytokine analysis

The level of pro-inflammatory cytokine IL-1β was investigated in cell-free BAL fluid supernatants from both sham and SLN-mApoE treated mice. Analysis was performed using a DuoSet ELISA kit for IL-1β (R&D Systems, Minneapolis, MN - USA) according to the manufacturer's protocol. Optical density was measured at 450 nm using FLUOStar Omega Multidetection Microplate reader.

2.13. Statistical analysis

Data were expressed as mean ± standard error of the mean (SEM) and analysed by Student's *t*-test. A p-value < 0.05 was considered significant.

3. Results and discussion

3.1. Physicochemical characterization of SLN

In the literature, various methods have been used to produce finely dispersed lipid nanoparticle suspensions [9], [40]. The warm microemulsion technique [41] allowed the easy preparation of fluorescently labelled SLN with different surface functionalization and characteristics (Table 1). The reaction between the thiol group at one terminal end of mApoE and the DPM located on the surface of SLN was exploited to functionalize SLN with mApoE. The covalent conjugation was performed in the pH range 6.5–7.5 in conditions that maintained the biological properties of the peptide. The physicochemical parameters of SLN were determined for each step of the conjugation procedure. The coupling efficiency between DPM and mApoE, assessed by fluorescence spectroscopy of tryptophan residue, was > 90%. A slightly increase in the average diameter of SLN was observed after the purification procedure both for SLN-mApoE and SLN-cys. Purified SLN-cys had a mean diameter of 121.5 ± 2.1 nm and a ζ-potential of − 62.4 ± 2.5 mV. SLN-mApoE had a mean diameter of 119.7 ± 2.5 nm and a ζ-potential of − 54.3 ± 2.1 mV. The negative ζ-potential of both SLN could contribute to prevent the particle aggregation increasing the stability of the dispersion by electrostatic repulsion.

Table 1. Characterization of DiO- and DiR-loaded SLN.

SLN	DPPA[c]	DPM[d]	Av. diam. [nm]	P.I.	Tripalmitin [rec.%]	PC[e] [rec.%]
DiO-DPPA-MAL BW[a]	10% molPC	0.4%molPC (DPM20)	120.0	0.235	86%	105%
DiO-DPPA-MAL AW[b]			103.7	0.236	85%	83%
DiR-DPPA-MAL BW	10% molPC	0.4%molPC (DPM20)	100.3	0.259	93%	111%
DiR-DPPA-MAL AW			99.68	0.279	92%	85%

a

Before washing.

b

After washing.

c

1,2-Dipalmitoyl-sn-*glycero*-3-phosphatidic acid.

d

1,2-Distearoyl-sn-*glycero*-3-phosphoethanolamine-*N*-[maleimide(polyethylene glycol)-2000].

e

Phosphatidylcholine.

3.2. Cytotoxicity and endocytosis of SLN

Cell toxicity induced by incubation of SLN with hCMEC/D3 was evaluated by means of PrestoBlue assay. hCMEC/D3 were incubated with increasing concentrations of SLN-cys or SLN-mApoE and the cell viability was assessed 24 h after the incubation. No reduction of cell viability was observed neither in presence of SLN-cys nor of SLN-mApoE, at any tested concentration (data not shown).

Time-dependent SLN-cell-interaction was assessed by FACS analysis. The cell-associated fluorescence increased over time for both SLN-mApoE and SLN-cys and values were about two-fold higher in presence of SLN-mApoE compared to SLN-cys, at each considered time point (Fig. 1).

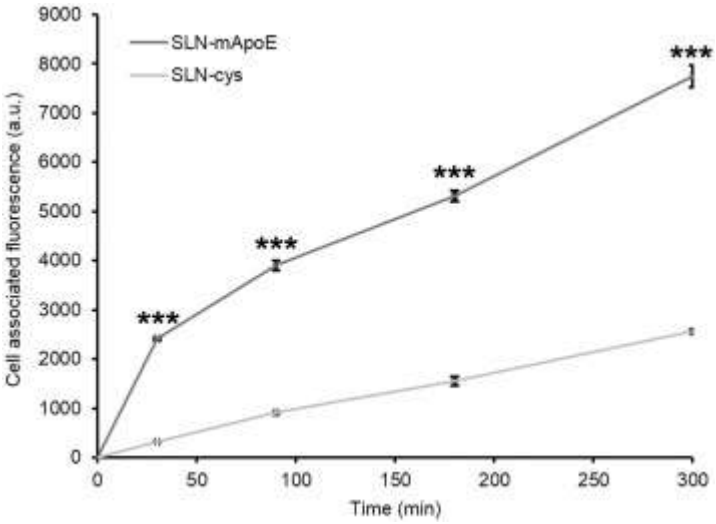

1. Download : Download high-res image (107KB)
2. Download : Download full-size image

Fig. 1. Time-dependent interaction of DiO-loaded SLN with hCMEC/D3. Cells were incubated with SLN-cys (light grey line) or SLN-mApoE (heavy grey line) for 30, 90, 180, 300 min and the cell-associated fluorescence was quantified by FACS analysis. Each value is the mean of three independent experiments; the SEM is presented as bars. ***$p < 0.001$ by Student's *t*-test.

The intracellular distribution of SLN-mApoE and SLN-cys was investigated by CLSM analysis. After overnight incubation with SLN-mApoE, green spots were observed below the plasma membrane and at the perinuclear region of hCMEC/D3, while in presence of SLN-cys a smaller amount of green fluorescence was detected into cells (Fig. 2A, B). SLN-mApoE did not co-localize neither with early/late endosomes and lysosomes, nor with Niemann-Pick C1 or Rab11 positive vesicles (Fig. 2C–F, red), thus prolonging SLN intracellular distribution within hCMEC/D3 cells, as also suggested for liposomes with the same surface functionalization [42]. The obtained Pearson's correlation coefficient (Rr) and Mander's colocalization coefficients for red (M1) and green (M2) are here reported: panel C Rr = 0.016, M1 = 0.058, M2 = 0.007; panel D Rr = 0.070, M1 = 0.023, M2 = 0.130; panel E Rr = − 0.095, M1 = 0.038, M2 = 0.043; panel F Rr = 0.077, M1 = 0.031, M2 = 0.069. SLN-cys did not co-localize with any of the investigated intracellular compartment (data not shown).

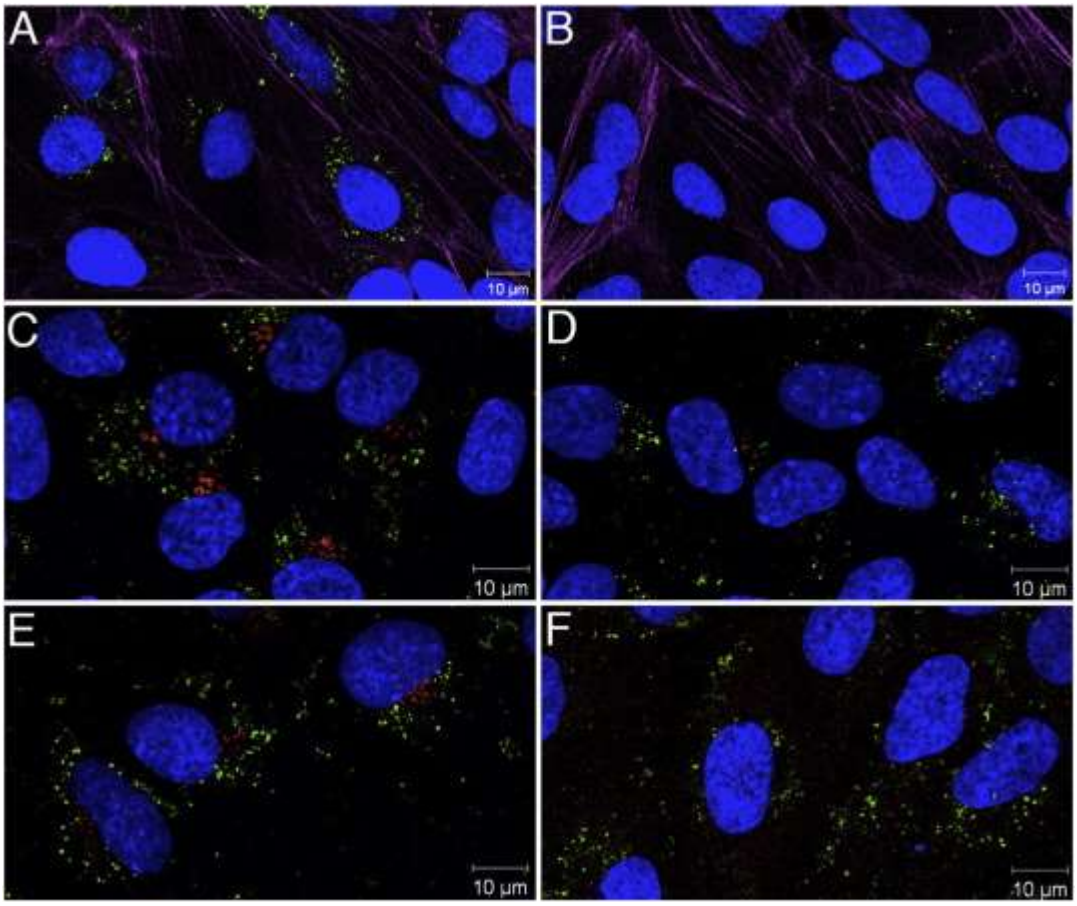

1. Download : Download high-res image (985KB)
2. Download : Download full-size image

Fig. 2. Cellular uptake and intracellular distribution of SLN in hCMEC/D3. Cells were incubated with DiO-loaded SLN-mApoE (A) and SLN-cys (B) overnight and the fluorescence was visualized by CSLM (green spots). The subcellular distribution of SLN-mApoE was evaluated by immunofluorescence staining of early endosomes (C), late endosomes/lysosomes (D), Rab11-positive vesicles (E) and Niemann-Pick C1 positive vesicles (F). Actin filaments were stained with Phalloidin 633 nm (magenta), nuclei were counterstained with DAPI (blue).

The here obtained results provide evidence that mApoE functionalization significantly improved SLN uptake by hCMEC/D3, according to data obtained with mApoE-functionalized liposomes [33], [34]. To explore the internalization pathways of SLN-mApoE in hCMEC/D3, cells were incubated with chlorpromazine to inhibit clathrin-coated pits development, filipin to hinder caveolae/lipid rafts transport through cholesterol-depletion, or with the macropinocytosis inhibitor amiloride to act on Na^+/H^+ exchangers. FACS analysis indicated that chlorpromazine reduced SLN-mApoE cell-associated fluorescence of 51% compared to control cells, while the incubation with filipine or amiloride led to a reduction of respectively 23% and 12%. The decrease of cell–associated fluorescence was statistically significant ($p < 0.01$) for all the chemical inhibitors employed. Therefore, our findings demonstrate that clathrin-mediated endocytosis plays a major role in SLN-mApoE uptake by hCMEC/D3. Nevertheless, a partial involvement of caveolae-mediated endocytosis, which are enriched in brain capillary endothelial cells [43], and of clathrin- and caveolae-independent mechanisms has been observed, thus supporting the hypothesis that multiple internalization mechanisms contribute to the cellular entry of SLN-mApoE [44]. Experiments on pathway mechanisms of entry were performed also with SLN-cys. The results showed little involvement of macropinocytosis, clathrin- and caveolae-mediated endocytosis to SLN-cys

interaction with hCMEC/D3. Indeed, the cell-associated fluorescence was unchanged for SLN-cys incubated with filipine, compared to control (cells incubated with SLN-cys without inhibitor). Amiloride reduced SLN-cys cell-associated fluorescence of 12%, while after treatment with chlorpromazine a 2% reduction of SLN-cys interaction with endothelial cells was observed.

3.3. SLN permeability across hCMEC/D3 monolayer

To assess SLN permeability across an in vitro BBB model dually radiolabelled formulations were prepared. The paracellular permeability of [^{14}C]-sucrose was evaluated to exclude alterations of the tight junction properties triggered by SLN. The EP value of [^{14}C]-sucrose was 1.5×10^{-3} cm/min both in presence and in absence of SLN, according to data already published for this BBB model [45]. As shown in Fig. 3, the functionalization of SLN with mApoE provided a higher permeability across the monolayer compared to SLN-cys. The EP values of [^{14}C]-DPPA were $5.7 \pm 0.3 \times 10^{-5}$ cm/min for SLN-mApoE and $0.6 \pm 0.09 \times 10^{-5}$ cm/min for SLN-cys. The EP values of [^{3}H]-CE were $6.9 \pm 0.4 \times 10^{-5}$ cm/min for SLN-mApoE and $0.5 \pm 0.08 \times 10^{-5}$ cm/min for SLN-cys. The ratio between the two radiotracers was maintained both in the upper chamber and in the lower compartment of the transwell system, thus suggesting that SLN-mApoE cross intact the cell monolayer as also indicated for liposomes on the same BBB model [33], [46]. The above EP values for SLN-mApoE are in agreement and higher than those previously reported by Bana and colleagues [39], who obtained EP values in the range of 2.01×10^{-5}–2.70×10^{-5} cm/min with brain targeted liposomes functionalized with the same modified sequence of ApoE, thus confirming mApoE as a promising ligand for BBB crossing. Together with the finding that SLN-mApoE did not co-localize with endosomes and lysosomes, these results support the hypothesis that, in analogy with LDL, SLN-mApoE could cross the BBB by transcytosis, bypassing the lysosomal degradation [43], [47].

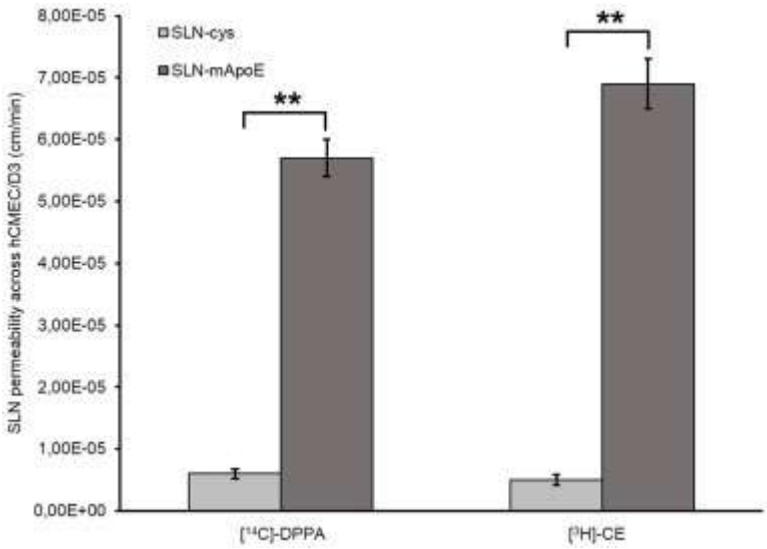

1. Download : Download high-res image (103KB)
2. Download : Download full-size image

Fig. 3. Transport of dually radiolabelled SLN across hCMEC/D3 monolayer. Cells were incubated with SLN-cys (light grey bars) or SLN-mApoE (heavy grey bars) at the final total lipid concentration of 0.1 mg/mL. The endothelial permeability (EP) of SLN was expressed as cm/min. Each value is the mean of three independent experiments. SEM is presented as bars. $^{**}p < 0.01$ by Student's *t*-test.

3.4. In vivo fluorescence molecular tomography imaging

The biodistribution assessment by means of fluorescence molecular tomography, thanks to its safety and ease of use, is a promising approach to investigate the localization of small molecule imaging agents or larger therapeutic biomolecules, i.e. nanoparticles, into organs and tissues [48]. Here, the in vivo imaging technique was exploited to study the influence of three different administration routes on SLN-mApoE bioavailability to the brain. DiR-loaded SLN-mApoE or SLN-cys were administered by IV and IP injection or IT instillation to healthy mice and the biodistribution was evaluated at different time points (Fig. 4).

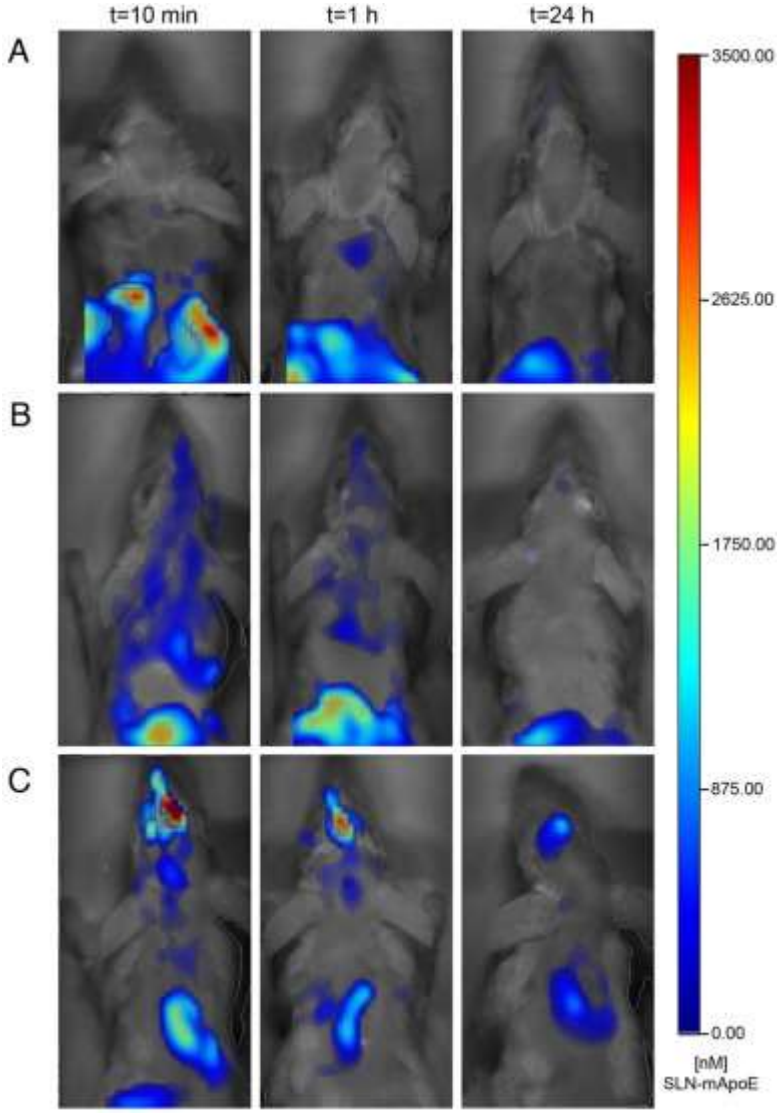

1. Download : Download high-res image (241KB)
2. Download : Download full-size image

Fig. 4. Biodistribution of DiR-loaded SLN-mApoE in healthy mice. SLN-mApoE at the final total lipid concentration of 10 mg/mL were intraperitoneally (A), intravenously (B) or intratracheally (C) administered to mice. Images were acquired 10 min, 1 h and 24 h after the treatment by FMT1500. (IP, intraperitoneal injection; IV, intravenous injection; IT, intratracheal instillation).

The amount of fluorescence in the brain was calculated by drawing a ROI corresponding to the whole brain volume of the mouse. After IP administration the fluorescence associated to SLN-cys

(data not shown) and SLN-mApoE was mainly limited to the abdominal cavity and no detectable signal was measured in the brain at any time (Fig. 4A). It is worth noting that at 3 h and 24 h after IV administration of SLN-mApoE the percentage of fluorescence reaching the brain was 0.15% and 0.06% of the injected dose, respectively. Interestingly, 3 h after IT instillation 4.52% of the administered dose was measured in the brain of SLN-mApoE treated mice. Moreover, SLN-mApoE showed a prolonged residence time in the brain. Indeed, 1.75% of the instilled dose was still detectable in the brain 24 h after the IT administration. These values were significantly higher ($p < 0.01$) compared to those of SLN-cys after IT administration (Table 2).

Table 2. Amount of fluorescence in the brain after intratracheal (IT) and intravenous (IV) administration of SLN-cys and SLN-mApoE.

Empty Cell		SLN-mApoE (n = 5)				SLN-cys (n = 5)			
		ROI [mm^3]	**DiR [pmol]**	**± SEM [pmol]**	**% of inj. dose**	**ROI [mm^3]**	**DiR [pmol]**	**± SEM [pmol]**	**% of inj. dose**
IT	3 h	1342.51	90.45	36.9	4.52	1338.80	27.71	3.39	1.38
	24 h	1335.54	35.04	15.96	1.75	1346.02	7.24	3.08	0.36
IV	3 h	1340.12	2.97	2.39	0.15	1346.12	13.35	4.66	0.67
	24 h	1337.37	1.31	0.95	0.06	1355.61	3.36	1.73	0.17

The quantification by FMT was performed at 3 h and 24 h to avoid overestimation due to the fluorescence still confined in the nanopharyngeal zone (after IT instillation, [36]) and in the bloodstream (after IV injection) at earlier time points. Interestingly, the brain fluorescence intensity associated to SLN-mApoE when administered IV is clearly lower compared to IT administration ($p < 0.01$), thus indicating a very low association of the fluorescence to the blood flow [48].

To exclude in vivo DiR release from SLN, 2 mice/group were treated with the free fluorophore by IT, IV or IP administration: 3 h and 24 h after IT instillation 1% and 0.2% of the instilled dose, respectively, was measured in the brain, while after IP and IV injections no detectable fluorescence was found in the brain. The different brain bioavailability of the free fluorophore compared to DiR-loaded SLN-mApoE supports the integrity of the latter, which therefore should be able to cross intact the air blood barrier after IT administration, and opens the possibility to further application of SLN-mApoE as delivery systems to improve the brain targeting of lipophilic drugs.

Recently, growing attention has been paid to the pulmonary region as a target for the delivery of macromolecules with systemic effect since the pulmonary route exhibits numerous benefits to be an alternative for repeated injection and oral administration, primarily due to the circumvention of the first pass effect and a lower concentration of drug-metabolizing enzymes in the lung [49], [50], [51], [52]. Moreover, the large surface area of the lungs, the thin epithelium of the respiratory zone (only 0.1 to 0.2 µm thick) and the enrichment of lymphatic and blood vessels of the pulmonary interstitium, make the lungs attractive as delivery route. Thanks to these properties, NPs can sedimentate or diffuse in the lungs according to the aerodynamic diameter and if they are able to escape the mucociliary clearance and the macrophage phagocytosis, their retention in the lung is prolonged [27]. Moreover, the alveolar region has the most permeable epithelium, thus allowing NPs to penetrate the thin cell layer and the interstitium, and supporting the translocation to other organs, including the brain [53]. We have not fully elucidated the fine mechanisms involved in SLN-mApoE lung to brain translocation yet, nevertheless there is evidence that transcellular pathways could play a major role in this process compared to paracellular transport, i.e. macrophage-mediated translocation [54]. Moreover we cannot exclude that SLN-mApoE could also be cleared from the lungs through a lymphatic route as indicated by Videira and colleagues [55].

Appropriate engineering of the designed NPs in terms of chemistry, size and surface charge for in vivo lung delivery is required to optimize the performance. The ability of SLN to travel across biological barriers due to its matrix lipid nature was assessed by Videira and colleagues [56]. The intrinsic properties of SLN-mApoE, such as their main diameter around 100 nm and their specific surface modifications that make them suitable for barrier crossing might explain their ability to translocate from the lungs toward the bloodstream thus targeting the brain. Indeed in our previous study we demonstrated that liposomes functionalized with mApoE peptide were able to cross an in vitro pulmonary epithelium model [36]. Lipka and colleagues investigated the biodistribution of PEG-modified gold nanoparticles (Au-PEG-NPs) following IT instillation and they demonstrated a prolonged retention of Au-PEG-NPs within the lungs with a minimal translocation toward the circulation. The small dimensions of Au-PEG-NPs (mean diameter of 10–30 nm) and above all their surface properties might explain the poor translocation from the lungs to the bloodstream and the authors themselves indicated other surface modifications, i.e. carboxylation, in order to promote greater potential to overcome the lungs barriers [57].

In our recent paper, we engineered liposomes (LIP) to investigate their fate in vivo and their ability to translocate from the lungs into the bloodstream, targeting the brain. It has been demonstrated the suitability and feasibility of the pulmonary administration route for delivering mApoE-PA-LIP to the brain and exerting their therapeutic effect in an animal model of Alzheimer's disease [36]. In the present study, by combining NP delivery through the pulmonary route [51], [52] and the sustained release properties of SLN, which have been extensively exploited for systemic opportunities [50], [58], we demonstrated an increased brain targeting of SLN-mApoE and a prolonged retention in the brain up to 24 h after the treatment. These results are in fully agreement with what we have previously reported for mApoE-PA-LIP [36]. Again, we believe that a low but constant amount of circulating SLN-mApoE slowly released from the lungs to the bloodstream, promotes interaction with the brain microvascular endothelium, thus enabling translocation of the SLN-mApoE to the brain. To the best of our knowledge, the here reported findings represent the first evidence of a comparative evaluation of three different administration routes of engineered SLN for the brain targeting, including the pulmonary route compared to IV and IP administration.

3.5. Bronchoalveolar lavage fluid analysis

We focused on the appropriateness of the pulmonary delivery technology such as design of SLN with no toxicity and the capability of accommodating both hydrophilic and hydrophobic drugs. Preclinical studies tended to support that lipid based carriers including liposomes, solid lipid nanoparticles and nanostructured lipid carriers are generally physiologically inert and biocompatible after inhalation, albeit no clinical safety data still available [55], [56], [58]. The feasibility of IT instillation as a route for SLN administration was assessed by BAL fluid analysis, in order to exclude inflammatory reactions triggered by SLN-mApoE persistence in the lungs. The differential count of the immune cells found in the BAL fluid proved that 24 h after IT instillation no significant differences in the percentage of AMs and PMNs (99% neutrophils) were found between sham and SLN-mApoE-treated mice. Moreover, the concentration of the cytokine IL-1β did not increase in treated mice (Table 3). Together our results suggest that pulmonary administration of SLN-mApoE does not induce alterations of the inner properties of the alveolar capillary barrier, creating a promising roadmap to deliver a large number of therapeutics into deep lung for both local and systemic effects [59].

Table 3. BALf profile in sham mice and SLN-mApoE IT treated mice.

Empty Cell	Sham (n = 5)		SLN-mApoE (n = 5)	
	Mean	± SEM	Mean	± SEM
AMs[a] [%]	82.58	14.14	64.25	11.86
PMNs[b] [%]	17.41	14.14	35.74	11.86
IL-1β [pg/mL]	25.23	8.99	26.94	14.44

a

Alveolar macrophages.

b

Polymorphonuclear leukocytes.

4. Conclusion

The transport of therapeutics across the BBB represents one of the main tasks for the treatment of neurological disorders. The employment of brain targeted SLN-mApoE and the exploitation of alternative administration routes to reach the brain could provide a strategy to overcome this obstacle. Indeed, i) the absence of cytotoxicity makes SLN very attractive candidates for brain delivery, ii) the warm microemulsion technique allows the easy preparation of SLN with mApoE as specific ligand for the brain targeting and iii) the pulmonary administration route of SLN-mApoE improves their brain bioavailability compared to parenteral administrations (IV and IP). It is expected that the increasing research interest in alternative administration routes will lead to more breakthroughs in several areas of both formulation and SLN design. Indeed, the absence of inflammatory phenomena in the lungs encourages further applications of this route for the targeted delivery of nanoscale systems to the brain, thus improving benefits to patients subjected to chronical treatments.

Acknowledgment

The research leading to these results has received funding from the European Community's Seventh Framework Program [FP7/2007-2013, grant number 212043 (NAD)]. The Authors report no conflicts of interest in this work. We thank Dr. Alfredo Cagnotto and Dr. Mario Salmona from IRCCS-Mario Negri Institute (Milano, Italy) for providing mApoE peptide, Prof. Paolo Blasi for his critical review of the manuscript and Dr. Mario Mauri for his support to CLSM co-localization analysis.

References

[1]

L. Zhang, F.X. Gu, J.M. Chan, A.Z. Wang, R.S. Langer, O.C. Farokhzad
Nanoparticles in medicine: therapeutic applications and developments
Clin. Pharmacol. Ther., 83 (2008), pp. 761-769, 10.1038/sj.clpt.6100400
Google Scholar

[2]

P. Blasi, S. Giovagnoli, A. Schoubben, C. Puglia, F. Bonina, C. Rossi, M. Ricci
Lipid nanoparticles for brain targeting I. Formulation optimization
Int. J. Pharm., 419 (2011), pp. 287-295, 10.1016/j.ijpharm.2011.07.035

Article
Download PDFView Record in ScopusGoogle Scholar

[3]
E.A. Neuwelt, N.J. Abbott, L. Abrey, W.A. Banks, B. Blakley, T. Davis, B. Engelhardt, P. Grammas, M. Nedergaard, J. Nutt, W. Pardridge, G.A. Rosenberg, Q. Smith, L.R. Drewes
Strategies to advance translational research into brain barriers
Lancet Neurol., 7 (2008), pp. 84-96, 10.1016/S1474-4422(07)70326-5
Article
Download PDFView Record in ScopusGoogle Scholar

[4]
P. Ballabh, A. Braun, M. Nedergaard
The blood-brain barrier: an overview: structure, regulation, and clinical implications
Neurobiol. Dis., 16 (2004), pp. 1-13, 10.1016/j.nbd.2003.12.016
Article
Download PDFView Record in ScopusGoogle Scholar

[5]
E.M. Cornford, S. Hyman
Blood-brain barrier permeability to small and large molecules
Adv. Drug Deliv. Rev., 36 (1999), pp. 145-163
Article
Download PDFView Record in ScopusGoogle Scholar

[6]
D. Paolino, D. Cosco, R. Molinaro, C. Celia, M. Fresta
Supramolecular devices to improve the treatment of brain diseases
Drug Discov. Today, 16 (2011), pp. 311-324, 10.1016/j.drudis.2011.02.006
Article
Download PDFView Record in ScopusGoogle Scholar

[7]
G. Tosi, L. Costantino, B. Ruozi, F. Forni, M.A. Vandelli
Polymeric nanoparticles for the drug delivery to the central nervous system
Expert Opin. Drug Deliv., 5 (2008), pp. 155-174, 10.1517/17425247.5.2.155
View Record in ScopusGoogle Scholar

[8]
P. Blasi, S. Giovagnoli, A. Schoubben, M. Ricci, C. Rossi
Solid lipid nanoparticles for targeted brain drug delivery
Adv. Drug Deliv. Rev., 59 (2007), pp. 454-477, 10.1016/j.addr.2007.04.011
Article
Download PDFView Record in ScopusGoogle Scholar

[9]
R.H. Müller, K. Mäder, S. Gohla
Solid lipid nanoparticles (SLN) for controlled drug delivery—a review of the state of the art
Eur. J. Pharm. Biopharm., 50 (2000), pp. 161-177
Article
Download PDFView Record in ScopusGoogle Scholar

[10]
M. Nassimi, C. Schleh, H.D. Lauenstein, R. Hussein, H.G. Hoymann, W. Koch, G. Pohlmann, N. Krug, K. Sewald, S. Rittinghausen, A. Braun, C. Müller-Goymann
A toxicological evaluation of inhaled solid lipid nanoparticles used as a potential drug delivery system for the lung
Eur. J. Pharm. Biopharm., 75 (2010), pp. 107-116, 10.1016/j.ejpb.2010.02.014

Article
Download PDFView Record in ScopusGoogle Scholar

[11]
S. Doktorovová, A.B. Kovačević, M.L. Garcia, E.B. Souto
Preclinical safety of solid lipid nanoparticles and nanostructured lipid carriers: current evidence from in vitro and in vivo evaluation
Eur. J. Pharm. Biopharm., 108 (2016), pp. 235-252, 10.1016/j.ejpb.2016.08.001
Article
Download PDFView Record in ScopusGoogle Scholar

[12]
M. Paranjpe, C.C. Müller-Goymann
Nanoparticle-mediated pulmonary drug delivery: a review
Int. J. Mol. Sci., 15 (2014), pp. 5852-5873, 10.3390/ijms15045852
View Record in ScopusGoogle Scholar

[13]
P. Ji, T. Yu, Y. Liu, J. Jiang, J. Xu, Y. Zhao, Y. Hao, Y. Qiu, W. Zhao, C. Wu
Naringenin-loaded solid lipid nanoparticles: preparation, controlled delivery, cellular uptake, and pulmonary pharmacokinetics
Drug Des. Devel. Ther., 10 (2016), pp. 911-925, 10.2147/DDDT.S97738
View Record in ScopusGoogle Scholar

[14]
P. Blasi, A. Schoubben, G.V. Romano, S. Giovagnoli, A. Di Michele, M. Ricci
Lipid nanoparticles for brain targeting II. Technological characterization
Colloids Surf. B: Biointerfaces, 110 (2013), 10.1016/j.colsurfb.2013.04.021
Google Scholar

[15]
V. Podio, G.P. Zara, M. Carazzonet, R. Cavalli, M.R. Gasco
Biodistribution of stealth and non-stealth solid lipid nanospheres after intravenous administration to rats
J. Pharm. Pharmacol., 52 (2000), pp. 1057-1063
View Record in ScopusGoogle Scholar

[16]
R.H. Müller, D. Rühl, S. Runge, K. Schulze-Forster, W. Mehnert
Cytotoxicity of solid lipid nanoparticles as a function of the lipid matrix and the surfactant
Pharm. Res., 14 (1997), pp. 458-462
View Record in ScopusGoogle Scholar

[17]
G. Tosi, B. Ruozi, D. Belletti
Nanomedicine: the future for advancing medicine and neuroscience
Nanomedicine (London), 7 (2012), pp. 1113-1116, 10.2217/nnm.12.90
View Record in ScopusGoogle Scholar

[18]
R.H. Edwards
Drug delivery via the blood-brain barrier
Nat. Neurosci., 4 (2001), pp. 221-222
View Record in ScopusGoogle Scholar

[19]
S. Wohlfar, S. Gelperina, J. Kreuter
Transport of drugs across the blood-brain barrier by nanoparticles
J. Control. Release, 161 (2012), pp. 264-273, 10.1016/j.jconrel.2011.08.017

Google Scholar
[20]
G. Tosi, B. Ruozi, M.A. Vandelli
Brain targeting with polymeric nanoparticles: which administration route should we take?
Nanomedicine (London), 8 (2013), pp. 1361-1363, 10.2217/nnm.13.135
View Record in ScopusGoogle Scholar
[21]
C.J. Cheng, G.T. Tietjen, J.K. Saucier-Sawyer, W.M. Saltzman
A holistic approach to targeting disease with polymeric nanoparticles
Nat. Rev. Drug Discov., 14 (2015), pp. 239-247, 10.1038/nrd4503
View Record in ScopusGoogle Scholar
[22]
M. Uner, G. Yener
Importance of solid lipid nanoparticles (SLN) in various administration routes and future perspectives
Int. J. Nanomedicine, 2 (2007), pp. 289-300
View Record in ScopusGoogle Scholar
[23]
S.A. Wissing, O. Kayser, R.H. Müller
Solid lipid nanoparticles for parenteral drug delivery
Adv. Drug Deliv. Rev., 56 (2004), pp. 1257-1272
Article
Download PDFView Record in ScopusGoogle Scholar
[24]
G.P. Zara, A. Bargoni, R. Cavalli, A. Fundarò, D. Vighetto, M.R. Gasco
Pharmacokinetics and tissue distribution of idarubicin-loaded solid lipid nanoparticles after duodenal administration to rats
J. Pharm. Sci., 91 (2002), pp. 1324-1333
Article
Download PDFView Record in ScopusGoogle Scholar
[25]
C. Puglia, P. Blasi, L. Rizza, A. Schoubben, F. Bonina, C. Rossi, M. Ricci
Lipid nanoparticles for prolonged topical delivery: an in vitro and in vivo investigation
Int. J. Pharm., 357 (2008), pp. 295-304, 10.1016/j.ijpharm.2008.01.045
Article
Download PDFView Record in ScopusGoogle Scholar
[26]
R. Cavalli, M.R. Gasco, P. Chetoni, S. Burgalassi, M.F. Saettone
Solid lipid nanoparticles (SLN) as ocular delivery system for tobramycin
Int. J. Pharm., 238 (2002), pp. 241-245
Article
Download PDFView Record in ScopusGoogle Scholar
[27]
S. Weber, A. Zimmer, J. Pardeike
Solid lipid nanoparticles (SLN) and nanostructured lipid carriers (NLC) for pulmonary application: a review of the state of the art
Eur. J. Pharm. Biopharm., 86 (2014), pp. 7-22, 10.1016/j.ejpb.2013.08.013
Article
Download PDFView Record in ScopusGoogle Scholar
[28]

C. Jaafar-Maalej, A. Elaissari, H. Fessi
Lipid-based carriers: manufacturing and applications for pulmonary route
Expert Opin. Drug Deliv., 9 (2012), pp. 1111-1127, 10.1517/17425247.2012.702751
View Record in ScopusGoogle Scholar

[29]
S. Azarmi, W.H. Roa, R. Löbenberg
Targeted delivery of nanoparticles for the treatment of lung diseases
Adv. Drug Deliv. Rev., 60 (2008), pp. 863-875, 10.1016/j.addr.2007.11.006
Article
Download PDFView Record in ScopusGoogle Scholar

[30]
J.C. Sung, B.L. Pulliam, D.A. Edwards
Nanoparticles for drug delivery to the lungs
Trends Biotechnol., 25 (2007), pp. 563-570, 10.1016/j.tibtech.2007.09.005
Article
Download PDFView Record in ScopusGoogle Scholar

[31]
M. Beck-Broichsitter, P. Kleimann, T. Gessler, W. Seeger, T. Kissel, T. Schmehl
Nebulization performance of biodegradable sildenafil-loaded nanoparticles using the Aeroneb Pro: formulation aspects and nanoparticle stability to nebulization
Int. J. Pharm., 422 (2012), pp. 398-408, 10.1016/j.ijpharm.2011.10.012
Article
Download PDFView Record in ScopusGoogle Scholar

[32]
M. Beck-Broichsitter, J. Gauss, C.B. Packhaeuser, K. Lahnstein, T. Schmehl, W. Seeger, T. Kissel, T. Gessler
Pulmonary drug delivery with aerosolizable nanoparticles in an ex vivo lung model
Int. J. Pharm., 367 (2009), pp. 169-178, 10.1016/j.ijpharm.2008.09.017
Article
Download PDFView Record in ScopusGoogle Scholar

[33]
L. Bana, S. Minniti, E. Salvati, S. Sesana, V. Zambelli, A. Cagnotto, A. Orlando, E. Cazzaniga, R. Zwart, W. Scheper, M. Masserini, F. Re
Liposomes bi-functionalized with phosphatidic acid and an ApoE-derived peptide affect Aβ aggregation features and cross the blood-brain-barrier: implications for therapy of Alzheimer disease
Nanomedicine, 10 (2014), pp. 1583-1590, 10.1016/j.nano.2013.12.001
Article
Download PDFView Record in ScopusGoogle Scholar

[34]
C. Balducci, S. Mancini, S. Minniti, P. La Vitola, M. Zotti, G. Sancini, M. Mauri, A. Cagnotto, L. Colombo, F. Fiordaliso, E. Grigoli, M. Salmona, A. Snellman, M. Haaparanta-Solin, G. Forloni, M. Masserini, F. Re
Multifunctional liposomes reduce brain β-amyloid burden and ameliorate memory impairment in Alzheimer's disease mouse models
J. Neurosci., 34 (2014), pp. 14022-14031, 10.1523/JNEUROSCI.0284-14.2014
View Record in ScopusGoogle Scholar

[35]
F. Re, I. Cambianica, C. Zona, S. Sesana, M. Gregori, R. Rigolio, B. La Ferla, F. Nicotra, G. Forloni, A. Cagnotto, M. Salmona, M. Masserini, G. Sancini

Functionalization of liposomes with ApoE-derived peptides at different density affects cellular uptake and drug transport across a blood-brain barrier model
Nanomedicine, 7 (2011), pp. 551-559, 10.1016/j.nano.2011.05.004
Article
Download PDFView Record in ScopusGoogle Scholar

[36]
G. Sancini, R. Dal Magro, F. Ornaghi, C. Balducci, G. Forloni, M. Gobbi, M. Salmona, F. Re
Pulmonary administration of functionalized nanoparticles significantly reduces beta-amyloid in the brain of an Alzheimer's disease murine model
Nano Res., 9 (2016), pp. 2190-2201, 10.1007/s12274-016-1108-8
View Record in ScopusGoogle Scholar

[37]
U. Bickel
How to measure drug transport across the blood-brain barrier
NeuroRx, 2 (2005), pp. 15-26, 10.1602/neurorx.2.1.15
Article
Download PDFView Record in ScopusGoogle Scholar

[38]
C. Tsurumi, N. Esser, E. Firat, S. Gaedicke, M. Follo, M. Behe, U. Elsässer-Beile, A.L. Grosu, R. Graeser, G. Niedermann
Non-invasive in vivo imaging of tumor-associated CD133/prominin
PLoS One, 5 (2010), Article e15605, 10.1371/journal.pone.0015605
View Record in ScopusGoogle Scholar

[39]
P. Mantecca, F. Farina, E. Moschini, D. Gallinotti, M. Gualtieri, A. Rohr, G. Sancini, P. Palestini, M. Camatini
Comparative acute lung inflammation induced by atmospheric PM and size-fractionated tire particles
Toxicol. Lett., 198 (2010), pp. 244-254, 10.1016/j.toxlet.2010.07.002
Article
Download PDFView Record in ScopusGoogle Scholar

[40]
N. Naseri, H. Valizadeh, P. Zakeri-Milani
Solid lipid nanoparticles and nanostructured lipid carriers: structure, preparation and application
Adv. Pharm. Bull., 5 (2015), pp. 305-313, 10.15171/apb.2015.043
View Record in ScopusGoogle Scholar

[41]
E. Marengo, R. Cavalli, O. Caputo, L. Rodriguez, M.R. Gasco
Scale-up of the preparation process of solid lipid nanospheres, part I
Int. J. Pharm., 205 (2000), pp. 3-13
Article
Download PDFView Record in ScopusGoogle Scholar

[42]
F. Re, I. Cambianica, S. Sesana, E. Salvati, A. Cagnotto, M. Salmona, P.O. Couraud, S.M. Moghimi, M. Masserini, G. Sancini
Functionalization with ApoE-derived peptides enhances the interaction with brain capillary endothelial cells of nanoliposomes binding amyloid-beta peptide
J. Biotechnol., 156 (2011), pp. 341-346, 10.1016/j.jbiotec.2011.06.037
Article

Download PDFView Record in ScopusGoogle Scholar

[43]
B. Dehouck, L. Fenart, M.P. Dehouck, A. Pierce, G. Torpier, R. Cecchelli
A new function for the LDL receptor: transcytosis of LDL across the blood-brain barrier
J. Cell Biol., 138 (1997), pp. 877-889
View Record in ScopusGoogle Scholar

[44]
A.A. Eltoukhy, G. Sahay, J.M. Cunningham, D.G. Anderson
Niemann-Pick C1 affects the gene delivery efficacy of degradable polymeric nanoparticles
ACS Nano, 8 (2014), pp. 7905-7913, 10.1021/nn501630h
View Record in ScopusGoogle Scholar

[45]
B. Poller, H. Gutmann, S. Krähenbühl, B. Weksler, I. Romero, P.O. Couraud, G. Tuffin, J. Drewe, J. Huwyler
The human brain endothelial cell line hCMEC/D3 as a human blood-brain barrier model for drug transport studies
J. Neurochem., 107 (2008), pp. 1358-1368
CrossRefView Record in ScopusGoogle Scholar

[46]
E. Markoutsa, K. Papadia, A.D. Giannou, M. Spella, A. Cagnotto, M. Salmona, G.T. Stathopoulos, S.G. Antimisiaris
Mono and dually decorated nanoliposomes for brain targeting, in vitro and in vivo studies
Pharm. Res., 31 (2014), pp. 1275-1289, 10.1007/s11095-013-1249-3
View Record in ScopusGoogle Scholar

[47]
A. Zensi, D. Begley, C. Pontikis, C. Legros, L. Mihoreanu, S. Wagner, C. Büchel, H. von Briesen, J. Kreuter
Albumin nanoparticles targeted with ApoE enter the CNS by transcytosis and are delivered to neurones
J. Control. Release, 137 (2009), pp. 78-86, 10.1016/j.jconrel.2009.03.002
Article
Download PDFView Record in ScopusGoogle Scholar

[48]
K.O. Vasquez, C. Casavant, J.D. Peterson
Quantitative whole body biodistribution of fluorescent-labeled agents by non-invasive tomographic imaging
PLoS One, 6 (2011), Article e20594, 10.1371/journal.pone.0020594
View Record in ScopusGoogle Scholar

[49]
R. Bi, W. Shao, Q. Wang, N. Zhang
Spray-freeze-dried dry powder inhalation of insulin-loaded liposomes for enhanced pulmonary delivery
J. Drug Target., 16 (2008), pp. 639-648, 10.1080/10611860802201134
View Record in ScopusGoogle Scholar

[50]
J. Liu, T. Gong, H. Fu, C. Wang, X. Wang, Q. Chen, Q. Zhang, Q. He, Z. Zhang
Solid lipid nanoparticles for pulmonary delivery of insulin
Int. J. Pharm., 356 (2008), pp. 333-344, 10.1016/j.ijpharm.2008.01.008

Article
Download PDFGoogle Scholar

[51]
J.S. Patton, P.R. Byron
Inhaling medicines: delivering drugs to the body through the lungs
Nat. Rev. Drug Discov., 6 (2007), pp. 67-74, 10.1038/nrd2153
View Record in ScopusGoogle Scholar

[52]
E. Seydoux, L. Rodriguez-Lorenzo, R.A. Blom, P.A. Stumbles, A. Petri-Fink, B.M. Rothen-Rutishauser, F. Blank, C. von Garnier
Pulmonary delivery of cationic gold nanoparticles boost antigen-specific CD4(+) T cell proliferation
Nanomedicine, 12 (2016), pp. 1815-1826, 10.1016/j.nano.2016.02.020
Article
Download PDFView Record in ScopusGoogle Scholar

[53]
G. Bachler, S. Losert, Y. Umehara, N. von Goetz, L. Rodriguez-Lorenzo, A. Petri-Fink, B. Rothen-Rutishauser, K. Hungerbuehler
Translocation of gold nanoparticles across the lung epithelial tissue barrier: combining in vitro and in silico methods to substitute in vivo experiments
Part. Fibre Toxicol., 12 (2015), p. 18, 10.1186/s12989-015-0090-8
View Record in ScopusGoogle Scholar

[54]
W.G. Kreyling, S. Hirn, W. Möller, C. Schleh, A. Wenk, G. Celik, J. Lipka, M. Schäffler, N. Haberl, B.D. Johnston, R. Sperling, G. Schmid, U. Simon, W.J. Parak, M. Semmler-Behnke
Air-blood barrier translocation of tracheally instilled gold nanoparticles inversely depends on particle size
ACS Nano, 8 (2014), pp. 222-233, 10.1021/nn403256v
View Record in ScopusGoogle Scholar

[55]
M.A. Videira, M.F. Botelho, A.C. Santos, L.F. Gouveia, J.J. de Lima, A.J. Almeida
Lymphatic uptake of pulmonary delivered radiolabelled solid lipid nanoparticles
J. Drug Target., 10 (2002), pp. 607-613, 10.1080/1061186021000054933
View Record in ScopusGoogle Scholar

[56]
M.A. Videira, A.G. Arranja, L.F. Gouveia
Experimental design towards an optimal lipid nanosystem: a new opportunity for paclitaxel-based therapeutics
Eur. J. Pharm. Sci., 49 (2013), pp. 302-310, 10.1016/j.ejps.2013.03.005
Article
Download PDFView Record in ScopusGoogle Scholar

[57]
J. Lipka, M. Semmler-Behnke, R.A. Sperling, A. Wenk, S. Takenaka, C. Schleh, T. Kissel, W.J. Parak, W.G. Kreyling
Biodistribution of PEG-modified gold nanoparticles following intratracheal instillation and intravenous injection
Biomaterials, 31 (2010), pp. 6574-6581, 10.1016/j.biomaterials.2010.05.009
Article
Download PDFView Record in ScopusGoogle Scholar

[58]

D. Cipolla, B. Shekunov, J. Blanchard, A. Hickey
Lipid-based carriers for pulmonary products: preclinical development and case studies in humans
Adv. Drug Deliv. Rev., 75 (2014), pp. 53-80, 10.1016/j.addr.2014.05.001
Article
Download PDFView Record in ScopusGoogle Scholar

[59]
N. Islam, V. Ferro
Recent advances in chitosan-based nanoparticulate pulmonary drug delivery
Nanoscale, 8 (2016), pp. 14341-14358, 10.1039/c6nr03256g
View Record in ScopusGoogle Scholar